

Multiwavefront digital holographic television

Malgorzata Kujawinska,^{1,*} Tomasz Kozacki,¹ Claas Falldorf,² Thomas Meeser,² Bryan M. Hennelly,³ Piotr Garbat,⁴ Weronika Zaperty,¹ Mikko Niemelä,⁵ Grzegorz Finke,¹ Marcin Kowiel,⁵ and Thomas Naughton^{5,6}

¹*Institute of Micromechanics and Photonics, Warsaw University of Technology, 8 Sw. A. Boboli St., 02-525 Warsaw, Poland*

²*BIAS - Bremer Institut für angewandte Strahltechnik GmbH Klagenfurter Straße 2, D - 28359 Bremen, Germany*

³*Department of Electronic Engineering, National University of Ireland, Maynooth, Co. Kildare, Ireland*

⁴*Institute of Microelectronics and Optoelectronics, Warsaw University of Technology, 75 Koszykowa St., 00-672 Warsaw, Poland*

⁵*University of Oulu, RFMedia Laboratory, Oulu Southern Institute, Vierimaantie 5, 84100 Ylivieska, Finland*

⁶*Department of Computer Science, National University of Ireland, Maynooth, Co. Kildare, Ireland*

*m.kujawinska@mchtr.pw.edu.pl

Abstract: This paper presents the full technology chain supporting wide angle digital holographic television from holographic capture of real world objects/scenes to holographic display with an extended viewing angle. The data are captured with multiple CCD cameras located around an object. The display system is based on multiple tilted spatial light modulators (SLMs) arranged in a circular configuration. The capture-display system is linked by a holographic data processing module, which allows for significant decoupling of the capture and display systems. The presented experimental results, based on the reconstruction of real world, variable in time scenes, illustrates imaging dynamics, viewing angle and quality.

©2014 Optical Society of America

OCIS codes: (090.2870) Holographic display; (090.4220) Multiplex holography; (090.1995) Digital holography.

References and links

1. H. J. Caulfield, ed., *The Art and Science of Holography: A Tribute to Emmeth Lieth and Yuri Denisyyuk* (SPIE Press, 2004).
2. I. Sexton and Y. Surman, "Stereoscopic and autostereoscopic display systems," *IEEE Signal Process. Mag.* **16**(3), 85–99 (1999).
3. J.-Y. Son and B. Javidi, "3-dimensional imaging systems based on multiview images," *J. Disp. Technol.* **1**(1), 125–140 (2005).
4. J. Hong, Y. Kim, H.-J. Choi, J. Hahn, J.-H. Park, H. Kim, S.-W. Min, N. Chen, and B. Lee, "Three-dimensional display technologies of recent interest: principles, status, and issues," *Appl. Opt.* **50**(34), H87–H115 (2011).
5. N. Hashimoto and S. Morokawa, "Real-time electroholographic system using liquid crystal television spatial light modulators," *J. Electron. Imaging* **2**(2), 93–99 (1993).
6. L. Onural, F. Yaraş, and H. Kang, "Digital holographic three-dimensional video displays," *Proc. IEEE* **99**(4), 576–589 (2011).
7. M. Sutkowski and M. Kujawinska, "Application of liquid crystal (LC) devices for optoelectronic reconstruction of digitally stored holograms," *Opt. Lasers Eng.* **33**(3), 191–201 (2000).
8. R. Häussler, A. Schwerdtner, and N. Leister, "Large holographic displays as an alternative to stereoscopic displays," *Proc. SPIE* **6803**, 68030M (2008).
9. M. Stanley, R. W. Bannister, C. D. Cameron, S. D. Coomber, I. G. Cresswell, J. R. Hughes, V. Hui, P. O. Jackson, K. A. Milham, R. J. Miller, D. A. Payne, J. Quarrel, D. C. Scattergood, A. P. Smith, M. A. Smith, D. L. Tipton, P. J. Watson, P. J. Webber, and C. W. Slinger, "100-megapixel computer generated holographic images from active tiling: a dynamic and scalable electro-optic modulator system," *Proc. SPIE* **5005**, 247–258 (2003).
10. J. Hahn, H. Kim, Y. Lim, G. Park, and B. Lee, "Wide viewing angle dynamic holographic stereogram with a curved array of spatial light modulators," *Opt. Express* **16**(16), 12372–12386 (2008).
11. F. Yaraş, H. Kang, and L. Onural, "Circular holographic video display system," *Opt. Express* **19**(10), 9147–9156 (2011).
12. T. Kozacki, M. Kujawinska, G. Finke, B. Hennelly, and N. Pandey, "Extended viewing angle holographic display system with tilted SLMs in a circular configuration," *Appl. Opt.* **51**(11), 1771–1780 (2012).
13. T. Kozacki, G. Finke, P. Garbat, W. Zaperty, and M. Kujawinska, "Wide angle holographic display system with spatiotemporal multiplexing," *Opt. Express* **20**(25), 27473–27481 (2012).

14. Y.-Z. Liu, X.-N. Pang, S. Jiang, and J.-W. Dong, "Viewing-angle enlargement in holographic augmented reality using time division and spatial tiling," *Opt. Express* **21**(10), 12068–12076 (2013).
15. J.-Y. Son, O. Chernyshov, M.-C. Park, W.-H. Son, B.-R. Lee, and J.-W. Kim, "A holographic display based on a Spatial Multiplexing," *Proc. SPIE* **8738**, 87380G (2013).
16. T. Kozacki, "On resolution and viewing of holographic image generated by 3D holographic display," *Opt. Express* **18**(26), 27118–27129 (2010).
17. T. Kozacki, M. Kujawińska, G. Finke, W. Zaperty, and B. Hennelly, "Holographic capture and display systems in circular configurations," *J. Disp. Technol.* **8**(4), 225–232 (2012).
18. T. Meeser, C. Falldorf, C. von Kopylow, and R. B. Bergmann, "Reference wave adaptation in digital lensless Fourier holography by means of a spatial light modulator," *Proc. SPIE* **8082**, 808206 (2011).
19. T. Kozacki, "Holographic display with tilted spatial light modulator," *Appl. Opt.* **50**(20), 3579–3588 (2011).
20. N. Pandey and B. Hennelly, "Compensation of reference beam sphericity in a multi-perspective digital holography based record-display setup," *Proc. SPIE* **8082**, 80822D (2011).
21. Y. Zhang, "Flexible camera calibration by viewing a plane from unknown orientations," in *Proc. of the Seventh IEEE International Conference on Computer Vision* (1999), pp. 666–673.
22. J. Heikkilä and O. Silven, "A four-step camera calibration procedure with implicit image correction," in *Proc. of the IEEE Computer Society Conference on Computer Vision and Pattern Recognition* (1997), pp. 1106–1112.
23. T. Tommasi and B. Bianco, "Computer-generated holograms of tilted planes by a spatial frequency approach," *J. Opt. Soc. Am. A* **10**(2), 299–305 (1993).
24. T. J. Naughton, Y. Frauel, B. Javidi, and E. Tajahuerce, "Compression of digital holograms for three-dimensional object reconstruction and recognition," *Appl. Opt.* **41**(20), 4124–4132 (2002).
25. T. J. Naughton, J. B. McDonald, and B. Javidi, "Efficient compression of Fresnel fields for Internet transmission of three-dimensional images," *Appl. Opt.* **42**(23), 4758–4764 (2003).
26. O. Matoba, T. J. Naughton, Y. Frauel, N. Bertaux, and B. Javidi, "Real-time three-dimensional object reconstruction by use of a phase-encoded digital hologram," *Appl. Opt.* **41**(29), 6187–6192 (2002).
27. M. J. Weinberger, G. Seroussi, and G. Sapiro, "The LOCO-I lossless image compression algorithm: Principles and standardization into JPEG-LS," *IEEE Trans. Image Process.* **9**(8), 1309–1324 (2000).
28. A. E. Shortt, T. J. Naughton, and B. Javidi, "Compression of digital holograms of three-dimensional objects using wavelets," *Opt. Express* **14**(7), 2625–2630 (2006).
29. A. E. Shortt, T. J. Naughton, and B. Javidi, "Histogram approaches for lossy compression of digital holograms of three-dimensional objects," *IEEE Trans. Image Process.* **16**(6), 1548–1556 (2007).
30. D. P. Kelly, D. S. Monaghan, N. Pandey, T. Kozacki, A. Michalkiewicz, G. Finke, B. M. Hennelly, and M. Kujawińska, "Digital holographic capture and optoelectronic reconstruction for 3D displays," *Int. J. Digit. Multimed. Broadcast.* **2010**, 759323 (2010).
31. L. Ahrenberg, A. J. Page, B. M. Hennelly, J. B. McDonald, and T. J. Naughton, "Using commodity graphics hardware for real-time digital hologram view-reconstruction," *J. Disp. Technol.* **5**(4), 111–119 (2009).
32. N. Delen and B. Hooker, "Free-space beam propagation between arbitrarily oriented planes based on full diffraction theory: a fast Fourier transform approach," *J. Opt. Soc. Am. A* **15**(4), 857–867 (1998).

1. Introduction

The holographic technique is based on the capture and display of 3D real world objects or scenes [1]. On the other hand current 3D TV stereoscopic and autostereoscopic imaging technique rely on 2D images only [1–3]. This simplification has enabled commercialization of 3D display techniques in the form of 3D cinema and television, however it does not allow the viewer to satisfy all cues of human visual 3D perception as is true in the case of holography [4,5]. Therefore 3D holographic video presents a very interesting development direction for 3D TV [4–7]. In holography the information contained in the object beam is recorded in a fringe pattern (hologram) which is produced by interference between the object and reference beams and thereby may be stored in the form of 2D images. Since the period of the fringes is inversely proportional to the angle formed by the object and reference beam, a process of recording and displaying a wide viewing angle scenes requires materials or optoelectronic devices with a high spatial resolution (more than 2000 lines/mm). Also the size (aperture) of the detector/display should be large enough to avoid the well-known "keyhole" problem, which limits the viewing zone of an reconstructed scene. Unfortunately the current state of technology does not allow development of the full holographic TV technology chain, including capture – transmission – processing and display, with high imaging quality for sufficiently big observation volumes as expected in commercial TVs. This is the effect of insufficient space bandwidth product (SBP) that can be currently captured by a single CCD/CMOS camera and displayed by a spatial light modulator (SLM).

In displays there are two main approaches to overcome this limitation: (i) reconstructing only a small part of a wavefront originating from an object (from a large volume of 3D scenes) and applying an eye tracking system supporting a single observer [8] and (ii) creating high resolution, big aperture (high pixel count) holographic display which provides simultaneously total information about a displayed image within a wide viewing zone for multiple observers [9]. The most natural way to increase the SBP in holographic systems is to create a larger display through combining reflective type Liquid Crystal on Silicon Spatial Light Modulators (LCSLMs) [10–14] or DMDs [15] into a flat or curved panel. The flat configuration has its limitation for extension of viewing angle for commercially available modulators [16]. Therefore, the circular configuration supported by spatiotemporal multiplexing is preferred [13, 17, 18].

However most published works are focused on holographic imaging of computer generated holograms or stereograms which have no restrictions or limitations connected with a data capture system. The big additional challenge is to provide an efficient digital holography approach from 3-D object data capture to wide viewing angle display of the image and to find a flexible method to couple capture and display systems. Also, in holographic television, the insufficient SBP is not the only concern. Huge amounts of data have to be transmitted from one place to another as fast as possible with unacceptable information loss in order to give the satisfactory viewer impression.

In the paper for the first time we present a holographic television system which addresses all the necessary features of a multi wavefront video system including: dynamic object capture, data compression, transfer and processing and finally 3D real world scene display. In Sections 2 and 3 the capture and display system configurations are explained in detail. Section 4 gives an overview of the calibration methodology for both systems, while in Section 5 all issues related to the implementation of the data transmission-processing line are discussed. Finally in Section 6 the functionality of the holographic video system was verified by transmission test where a holographic capture of 3D dynamic scene was performed in Bremen, Germany, while holographic display in Warsaw, Poland.

2. Capture system

The capture system consists of six wave field (holographic) sensors, that allow simultaneous capture of a set of frames recording wide angle object information. Such a set of holographic HD frames creates a single multi wavefront frame (MWF), which is then transferred and processed in the video system.

The physical realization of the multi CCD holographic capture system was developed by Bremen Institute of Applied Beam Technology (BIAS). The system is in a partial circular six-sensor arrangement with a capability to capture digital holographic videos of dynamic scenes from six different views simultaneously as shown in Fig. 1. The high pulse energy laser InnoLas YM-R 800 with the wavelength 532nm, a pulse length of 6ns, a maximum pulse energy of 100mJ and maximum repetition rate 10Hz was chosen as the light source. Since the energy of the laser is too high to apply fibers the reference waves and the object illuminating wave are guided by beam splitters plates and mirrors, whereby the reference light path length of one sensor can strongly differ from the reference light paths of the other sensors and the object light path. However the coherence length of the laser is sufficient and equals approx. 120cm. In order to shape six plane reference waves illuminating each CCD entirely, a collimator is placed in front of the pulsed laser right before splitting the reference wave into six reference waves. All six reference waves impinge perpendicularly onto the CCDs to provide an in-line digital Fresnel holography capturing setup. A neutral density filter has been positioned in the reference wave arm (before it is separated into the six reference waves) and a second one in the object wave arm in order to control the relation between the object wave power and the reference wave power by varying those filters. Each CCD provides 2056 pixels in the horizontal and 2452 pixels in the vertical direction with a pixel pitch of $\Delta_1 = 3.45\mu\text{m}$ in

both directions, where the subscript $_1$ relates capture system. However the utilized image size of each hologram was reduced to 1920 (width) x 1080 (height) pixels with 8 bit per pixel in order to match the resolution of the SLMs in the display. The exposure time of each CCD was set to 100ms, but the real capturing time is just 6ns due to the pulse length of the laser. To synchronise the capturing time of the six sensors a trigger device was connected to the six CCDs. All sensors are controlled by one computer, the Main PC. This PC merges the captured digital holograms into one HDF5-file, which we named as the multi wavefront frame (MWF), compresses the data and transmits to the display side. The full process is automated.

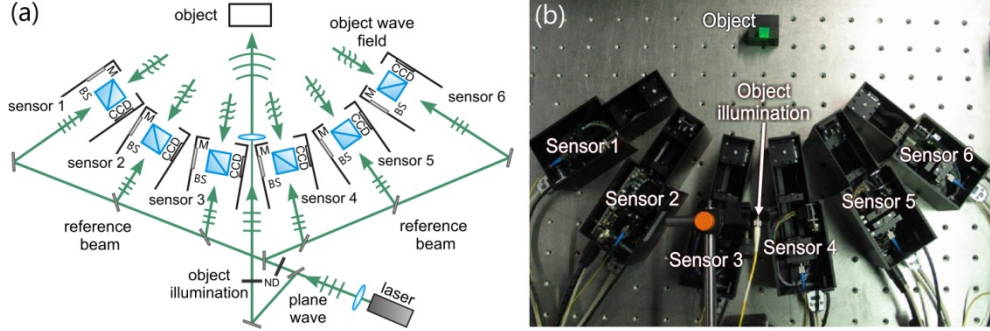


Fig. 1. The digital holographic capture system: (a) the scheme and (b) the photo of the setup.

The described sensor system was used for capturing six digital holograms of a dynamic scene from different perspectives. In order to show the full functionality of the capture system holograms of a sample object were reconstructed numerically. The object was a watch running in real time. The numerical reconstructions of the six digital holograms captured at the same moment are shown in Fig. 2. These reconstructions illustrate the images of the watch as seen from different perspectives, the rectangular zero diffraction order is clearly visible centered in the image, and the cloudy twin image is also visible. The coinciding positions on the hands of the clock document the synchronism of the capture.

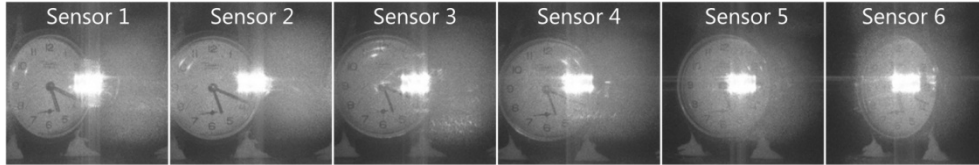


Fig. 2. Numerical reconstructions of digital holograms of a watch captured by different sensors at the same time.

The position of the object within the captured scene is slightly different at each hologram due to misalignments of the optical components of the sensors. This indicates the need of a calibration method to correspondingly align the six displays on the reconstruction side. The calibration method is described in the Section 4. Due to constraints specified by the capturing arrangement, the capture is subjected to the following restrictions:

- the object size h is limited by the wavelength λ , the pixel pitch $\Delta_1 = 3.45\mu\text{m}$ of the CCDs, and the distance z between the axis of rotation of the partial circular arrangement and the capturing CCDs (here $R = z_1 = 260\text{mm}$). Applying the equation:

$$h_1 = \frac{z_1 \cdot \lambda_1}{\Delta_1}, \quad (1)$$

a maximum object size of 40mm is obtained for the given capturing arrangement:

- the gap size: due to the dimensions of the sensor housings, the six CCDs detect a smaller part of the wave field than the whole partial circular six-sensor arrangement covers. This

leads to a gap in between the captured digital holograms of the different sensors. This gap together with the distance between the axis of rotation of the partial circular arrangement and the CCDs, allows us to determine the angular gap between captures. Taking into account the capturing setup ($R = 260\text{mm}$) and the width of the used CCD (6.6mm, because 1920 pixels are addressed only), each CCD detects an angular range of approx. 1.5° in the horizontal direction. However the angle between the axes of two neighboring CCDs in this direction is approx. $15^\circ \pm 1^\circ$. This results in a minimum gap between two neighboring CCDs of at least 13.5° and the corresponding capture fill factor $FF_l = 0.1$,

- the capturing frame rate is limited by the maximum pulse rate of the employed pulsed laser, which is 10Hz. However, the actual maximum frame rate could be even lower depending on the total recorded data and the transmission bandwidth. The pixel number of the employed CCDs is 2056 (width) x 2452 (height) pixels. Using all of these pixels the capturing frame rate was below that of the laser pulse. However to increase the speed of the transmission-processing line the CCDs were addressed with a decreased pixel number (1920 x 1080) matching the SLM pixel number. The usage of the decreased pixel number in the capturing process results in a maximum capturing frame rate of 9.8fps which is nearly the maximum frame rate of laser pulse.

As described above the capture system with multiple cameras provides holographic data of a real world varying in time 3D object or scene. The data will be used as the input for the tests of the full technology chain of holographic 3D video. However the main disadvantage of this capture system is the low value of capture fill factor. The reconstructed images will not provide a continuous object optical field, which will directly influence the comfort of observation.

3. Display system

The parameters of the display system have to be coupled opto-mechanically and numerically with the capture system, so that it can properly display a 3D image of an object or scene. This requirement is fulfilled by a holographic display system based on six phase LCSLMs. The SLMs are aligned on a circle of twice the radius of the reconstruction distance. The scheme and photo of the display are shown in Fig. 3. The display is an assembly of two modules: illumination and reconstruction. The task of the first one is to illuminate SLMs with a set of parallel, homogeneous, coherent and linearly polarized beams (we use here CWNdY laser with a wavelength of 532nm). Also, the illumination module provides vertically tilted beams necessary for a separation of incident and reflected beams (the tilt is small approx. 1.5°). In the reconstruction module there are six SLMs, which are tilted in the horizontal direction with respect to the illumination beam. This tilt enables the use of a simple illumination configuration, simultaneously coupling the capture-display systems.

The major feature of display circular configuration is its extended (through spatial multiplexing) viewing angle and horizontal parallax. However, in the vertical direction there remains a small viewing angle which is problematic for a comfortable perception of reconstructed images. For this reason we place an asymmetric diffuser in the reconstruction plane which extends the size of an observed image in vertical direction. The diffuser scatters light approximately in one direction only (y) and plays the role of a scattering medium which at the cost of removing vertical parallax extends the size of the observable image.

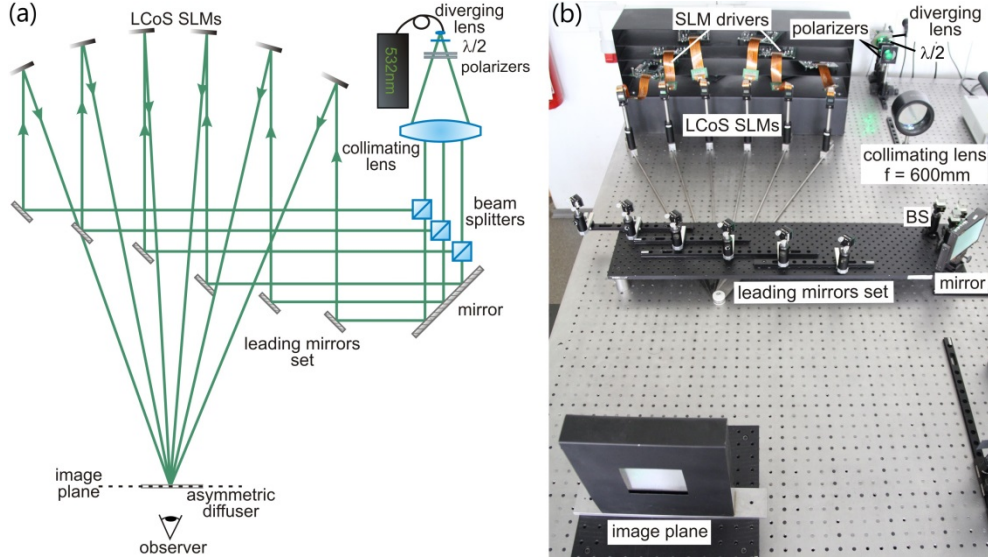


Fig. 3. The digital holographic display: (a) the scheme and (b) photo.

There are two major differences in the configurations of the capture and display setups. At first there is a difference in the pixel pitch sizes of the CCD ($\Delta_1 = 3.45\mu\text{m}$) and SLM ($\Delta_2 = 8\mu\text{m}$), where the subscript $_2$ concerns parameters in the display system. Secondly, the display SLMs have different angular tilts in respect to optical axis then the CCDs of capture system.

The difference in pixels has a minor effect; it simply redefines the geometry of the circular display arrangement with respect to the capture one via magnifications: transverse ($m_t = 2.319$), longitudinal ($m_l = 5.38$), and angular ($m_a = 0.43$) [17]. In the display system, the SLMs are aligned in a circular arrangement of radius $R = z_1 = 1.43\text{m}$ with an angular pitch of 6.39° . The increase in reconstruction distances gives a proportional increase of the viewed area (linear Field of View $FoV = \lambda_2 z_2 \Delta_2^{-1} = 95\text{mm}$) and drop of single x -directional SLM viewing angle to 0.61° . This small viewing angle, in comparison to angular pitch, gives inconvenient observation conditions. For example for an observation distance of 500mm the reconstructed images are seen as 4mm wide stripes separated by 33.2mm [17]. The second difference is related to the different angular tilts of SLMs vs. CCDs, it requires the usage of an additional algorithm in the data processing chain, so when a plane wave is diffracted at a tilted SLM, the correct object wave is generated at the correct angle. The tilts of SLMs are small ones, tilt of marginal SLM is approx. 8° . For such a tilt calibration curves, which are measured for normal orientation of SLM can be applied [19].

The display system is linked with the capture system via a data transfer processing platform and the SLMs are driven by computer with a processing platform ensuring synchronized display of the transmitted holographic MWFs.

4. Capture-display system's mutual calibration

All images obtained from a set of 6 digital holograms have to be reconstructed in the same 3D image coordinate system. To achieve this, a two-step calibration procedure is implemented:

Step 1: determination of the CCD positions and orientations based on recording a known flat chessboard object with a well-defined size and a number of clearly distinguishable features (Fig. 4). The first stage is to measure and compensate for any spherical aberration in the six reference beams that might affect our measurement [20]. Then each CCD records a hologram of a static chessboard object with ten different diffuser illuminations allowing ideal speckle noise reduction by averaging of the reconstructed intensities. The resulting images are

input to an open source camera calibration algorithm, developed in Caltech, based on methods outlined in [21, 22]. The standard deviation of the error of cameras orientation was estimated to be 0.31 degrees.

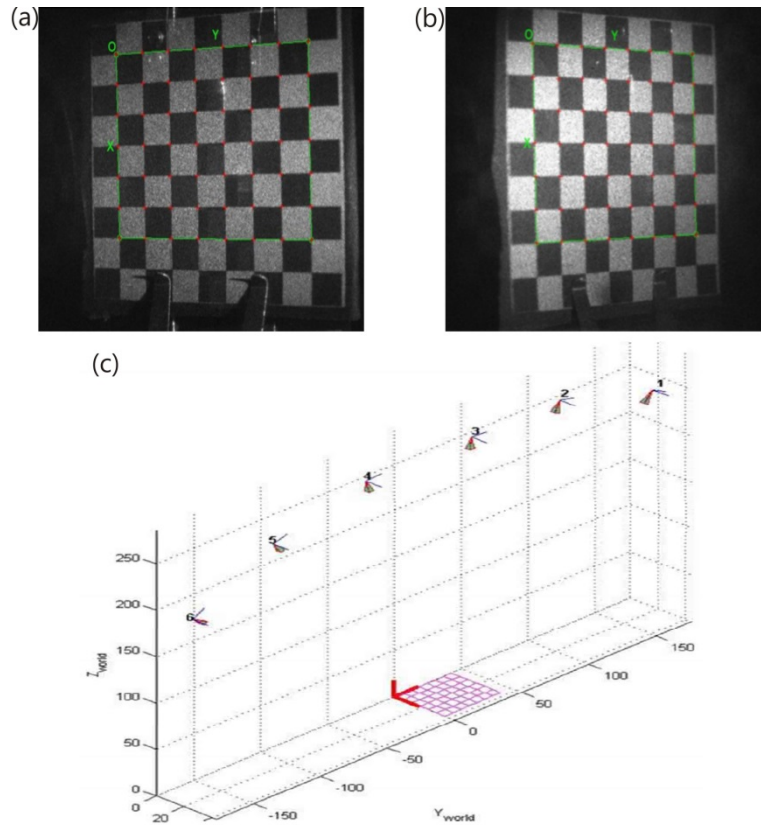


Fig. 4. Illustration of capture system calibration, image of calibration target from (a) most right “1” and (b) most left “6” CCD; (c) CCD positions and orientations calculated from six recordings (axes in mm).

Step 2: aligning the positions and orientations of the SLMs in the display set to match the CCD positions. It is based on calculating a computer generated hologram for each SLM (with a given 3D position and orientation) which will reconstruct the same 3D scene. An algorithm is designed to create a CGHs of a cross hair target on a tilted plane (Fig. 5(a)) using the method presented in [23]. The example numerical reconstructions of two of the CGHs are shown in Figs. 5(b) and 5(c). After an approximate positioning, the SLMs are adjusted sequentially until the reconstructions overlap. We note that in this study no attempt was made to coherently stitch the wavefields from each SLM together which would require alignment in the order of $\ll \lambda$.

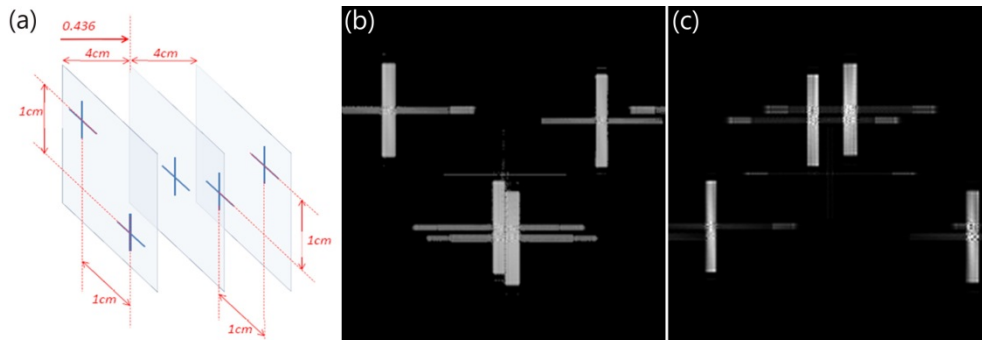


Fig. 5. (a) The 3D scene with five cross hairs on three planes; (b) Numerical reconstruction of CGH for (b) left most and (c) right most SLM. The centre cross hair is difficult to see because it is very narrow.

5. Data transfer-processing platform

Data flow within the holographic multi wavefront television system from capture to display is illustrated in Fig. 6. Data coding ensures a common representation for the data. Compression C is required to speed up the data transfer between capture and display locations, and processing is required to reduce noise (remove zero order, twin image and speckle noise), convert the hologram intensities to phase wavefronts, and to adapt the wavefronts to the specific arrangement of LCSLMs devices in the display.

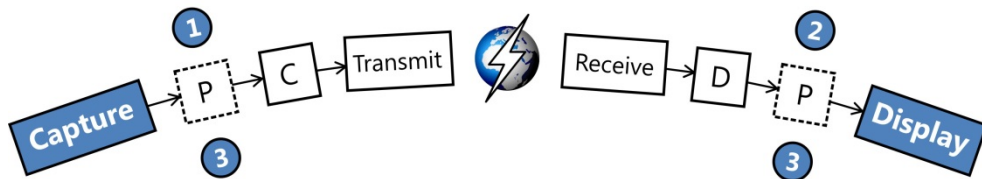


Fig. 6. The data flow in the holographic television system. The numbers determine the alternative location of data processing: (1) on the capture side, (2) on the display side, or (3) partially on both sides; P, C, and D denote processing, compression, and decompression, respectively.

It is assumed that compression needs to take place immediately before transmission, and decompression should take place immediately after transmission. There are three general options for combining compression, transmission, and digital processing functionalities, as illustrated in Fig. 6. There are several options for the location of the data processing module:

- option (1) allows a simpler display side architecture, and facilitates the efficiency that only the real-valued phase data will be transmitted rather than the larger corpus of raw hologram data. However, in this case the full details of the display architecture needs to be known *a priori*.
- option (2) allows decoupling of the capture and display, so that in principle several different display technologies could use the same capture side. Additionally conventional coding/compression algorithms can be applied for intensity data.
- option (3) finds a compromise, for example performing twin removal and noise reduction on the capture side and display-specific processing on the display side, but may require the overhead of transmitting complex valued wavefront data.

Every important requirement in conventional television or video is decoupling of the capture and display systems. This was also the main reason for choosing option (2) for the multi wavefront holographic television system described herein. It also allows us to apply at the capture side, a conventional personal computer with special C++ software for creating

MWFs. At the display side a computer with software on multi-GPUs is employed in order to ensure that full hologram processing is performed in a reasonable time.

5.1 Coding, compression and transfer

Fast Ethernet is used for live transmission of digital holographic videos to the display side. Bandwidth was limited to a maximum of 12.5MBytes per second. Using six CCDs with an image size of 1920x1080 pixels each leads, without data compression, to a theoretical frame rate of 1fps at most. Practically, the real bandwidth achieved is about 8MBytes per second, yielding a maximum frame rate of 0.6fps.

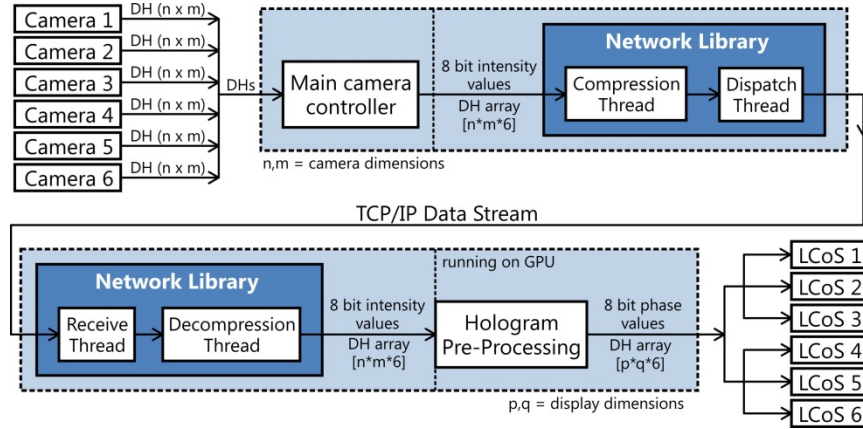


Fig. 7. Overview of the data manipulation and transfer stages between capture and display.

We created a software integration framework with the C++ programming language with which to provide support for each of the operational components in the full chain from capture to display (Fig. 7). The operational components were capture control, hologram compression, data transmission, data receiving, hologram decompression, data processing, and display control.

Coding was restricted to processes that did not change the fundamental syntax of the data (i.e. no explicit decoding was required on the display side). This allowed algorithms designed to process holograms directly from digital camera outputs to be reused on the display side. The DC was removed to lower the effective dynamic range of the hologram prior to quantization, and holograms captured simultaneously were concatenated. The hologram from each camera had dimensions 1920×1080 pixels and 8 bits of unsigned integer hologram data in each pixel, and the full frame representing all data captured at time t_0 was a multi wavefront frame with dimensions $6 \times 1920 \times 1080$ pixels of 8-bit signed integer values.

Compression was effected by a QoS (quality of service) algorithm that was devised to gracefully decrease the quality of the hologram data if the requested frame rate is increased by a user at the display side [24, 25]. It consisted of removing blocks of pixels at the edges of the holograms that would have less subjective influence on the display field of view. Next, uniformly quantizing the remaining pixels from their original 8-bits to something lower, as it was shown that relatively few bits of information are required to generate acceptable phase-only hologram reconstructions [26]. Finally, applying a lossless encoder that could take advantage of two-dimensional spatial redundancy. For this we chose a variant of the JPEG-LS lossless standard for continuous-tone images [27]. While such an approach will achieve less impressive compression ratios compared with more established techniques [28, 29], it allows fine control of the file size, and facilitates very fast implementation. Compression time is an important consideration after compression ratio for online networking applications.

It was decided to use conventional TCP/IP communications and the standard existing internetwork infrastructure at both capture and display institutions. On the capture side, the

software for coding, compression, and networking was compiled with the camera control routines into a single software application. On the display side, a single software application combined networking, decompression, processing on graphics processors, and directly mapping the phase images to the LCSLM devices. An user interface on the display side allowed analysis of the underlying network, analysis of congestion and dropped frames somewhere in the framework, and requests for increased/decreased compression ratio to be sent to the display side.

5.2 Data processing

The holographic capture system uses the in line Fresnel architecture. One of the main reasons for the choice of the in-line set up was the similarity of the capture architecture to the display one and the availability of an algorithm which was shown to successfully remove the deleterious effects of the twin image and DC terms [30]. This algorithm reduces the DC terms by high pass filtering the hologram and reduces the twin image term by propagating to the twin image plane, removing the in focus twin image by thresholding and propagating back to the hologram plane.

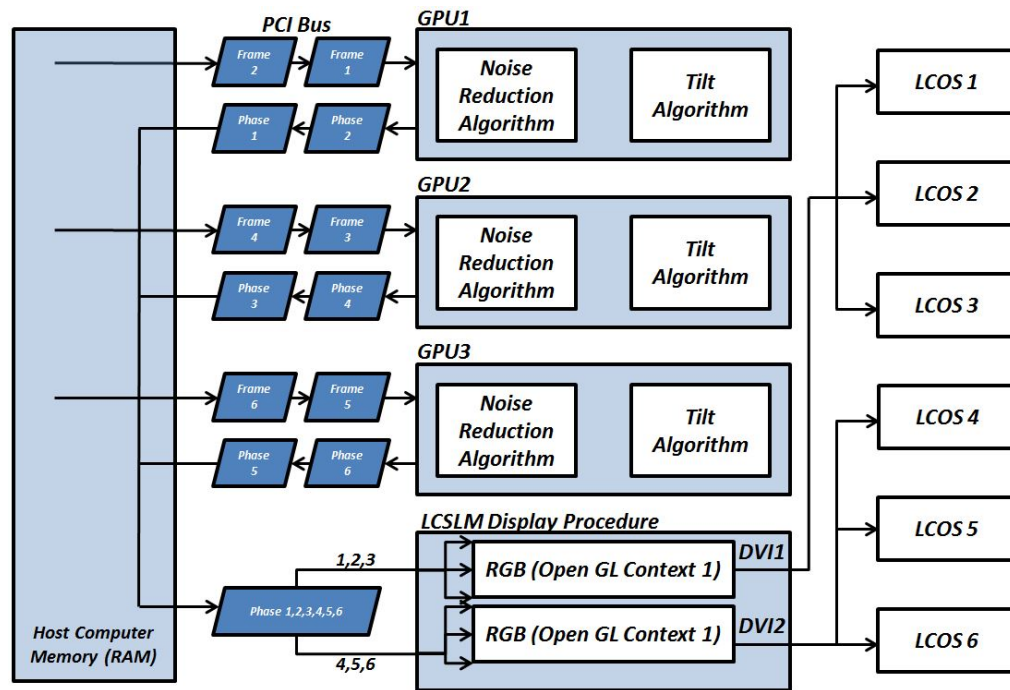


Fig. 8. GPU Processing and data transfer after decompression.

Our noise reduction algorithm consists of the algorithm proposed in [30] with a number of advancements; firstly an autofocus algorithm detects the most in focus plane for the twin image and secondly a refined filtering procedure is applied. This involves firstly numerical propagation to the real image plane and removing the in focus energy by thresholding, followed by back propagation to the hologram plane. Secondly we numerically propagate to the twin image plane where a binary mask of the in focus twin image is obtained with reduced noise from the out of focus twin image. Finally, this improved binary mask is used in the algorithm proposed in [30]. In total the filtering procedure employs seven FFT algorithms to filter each hologram. For this reason a GPU (Graphics Processing Unit) solution was sought for implementation of the numerical processing. It has been shown that GPU implementation of the FFT algorithm offers a significant speed up over CPU [31]. We note we found that the

algorithm worked best when the object did not occupy the entire reconstruction window. Sparse objects allowed for removal of the entire twin image term while removing only a small part of the real image term in the process. We note that input to the noise reduction algorithm is the pixel data of the CCD, having been previously compressed, transferred and decompressed. Output of the noise reduction algorithm is a complex image, which has been calculated by removing the DC and twin image terms from the hologram.

The tilt algorithm follows, which is required due to the effect of the difference of the geometry of the plane of the CCD during capture and plane of the SLM in the display, i.e. the LCOS is tilted with respect to the corresponding CCD. The noise reduction algorithm provides a complex valued image as input to the tilt algorithm. These complex images are processed using a computational diffraction method to compute the tilted display geometry. The algorithm applies a rigorous propagation of the paraxial field between two tilted planes [19, 32] and consists of computation of FFT, spectrum interpolation as a function of tilt and an IFFT. Only the phase values are given as output of the algorithm, after quantizing to 256 gray scale values which is the required format for the LCOS driver.

As shown in Fig. 8 we employ three NVIDIA G200 GPUs in parallel to perform the processing stage. First two of the six decompressed CCD frames are sent serially across the PCI bus to each of the three GPUs. Each GPU processes two frames using the two algorithms described above and outputs two 256 level phase images. Finally six outputs are merged into two RGB signals, which are buffered in Pixel Buffer Object (PBO). PBO is connected with the texture object which is displayed at the LCSLM's. The final element of processing path (Fig. 8) ensures that the display of two separate RGB buffers is synchronized. This is programmed in two separate threads using a swap barrier mechanism to synchronize the swaps of multiple LCSLM's buffer (OpenGL context) without special hardware support.

6. Experimental results of the transmission test

The functionality of the developed full technology chain of multi wavefront television system is presented experimentally, at first by showing the achieved frame rates and then by assessing the imaging quality that was obtained. In order to check the efficiency of the technology chain a speed test was implemented. During the test several Bremen – Warsaw transmissions were executed where the achieved frame rates were measured. The value of the frame rate is a result of the timings of compression, internet transmission, decompression, filtering, tilt removal and display of six high definition (1920 x 1080 pixels) holograms, since our system is based on multi wavefront frames. The transmissions were performed for different software configurations, which includes the use of different algorithms for compression and noise reduction. The results obtained (“Full chain”) are compared with frame rates specified by the execution speed of the developed GPU platform and these are indicated as “Local”. The frame rates achieved are summarized in Table 1, in each table field the values of frame-rates achieved using software executing on a single GPU and on multiple GPUs is shown. Based on these tests three main limitations of the operation speed are found:

- flow capacity of available network for Bremen – Warsaw connection, gives a maximum speed limit of 0.38Hz,
- compression and decompression procedures, the most efficient JPEGLS algorithm limits speed to 1.89 Hz,
- MultiGPU solution of processing procedures (DC and twin removal) gives speed limitation of ~2.46 Hz,
- the speed of processing procedures can be increased to 10 Hz by application of off axis holograms.

Table 1. The frame rates for SingleGPU / MultiGPU solutions

| Processing | | Compression | | | |
|--------------|------------|---------------|------------|-------------|---------------|
| | | Without ~100% | Bzip2 ~70% | JPEGLS ~50% | uqJPEGLS ~50% |
| Segmentation | Full chain | 0.1/0.13 | 0.3/0.28 | 0.32/0.3 | 0.34/0.38 |
| | Local | 0.62/2.46 | 0.46/0.46 | 0.62/1.89 | 0.62/1.6 |
| Off Axis | Local | 1.32/10.07 | 0.46/0.46 | 1.32/1.87 | 1.33/1.49 |

Figure 9 presents exemplary reconstructions for two scenes: watch and chicks. For both captured scenes Fig. 9 shows two exemplary multiwavefront frames MWFs as reconstructed by separate SLMs 1-6. During the scenes capture, the watch and chicks objects were placed on a rotating table in order to introduce changes in time. The respective time sequence of reconstructed images are shown by (Fig. 9 and [Media 1](#)) and (Fig. 9 and [Media 2](#)). Specifically, [Media 1](#) illustrates time synchronization of watch scene, while [Media 2](#) illustrates real-time interaction of an additional object with the chick scene. The Fig. 2 shows numerical reconstructions of the full MWF for the same watch scene. This enables qualitative comparison of imaging quality for both numerical and optical reconstructions, which we believe is very similar. In order to show that the 6 images created by 6 separate SLMs are properly adjusted in the holographic display we present the videos (Fig. 9 and [Media 3](#)) of the wide viewing angle (combined from all SLMs) images of static and running watch as seen by an observer through asymmetric diffuser.

The views illustrate imaging synchronization, dynamics, viewing angle of the system and imaging quality for the applied “Full chain” processed with uqJPEGLS compression. There are visible effects of residues of the zero order and aliasing for large objects.

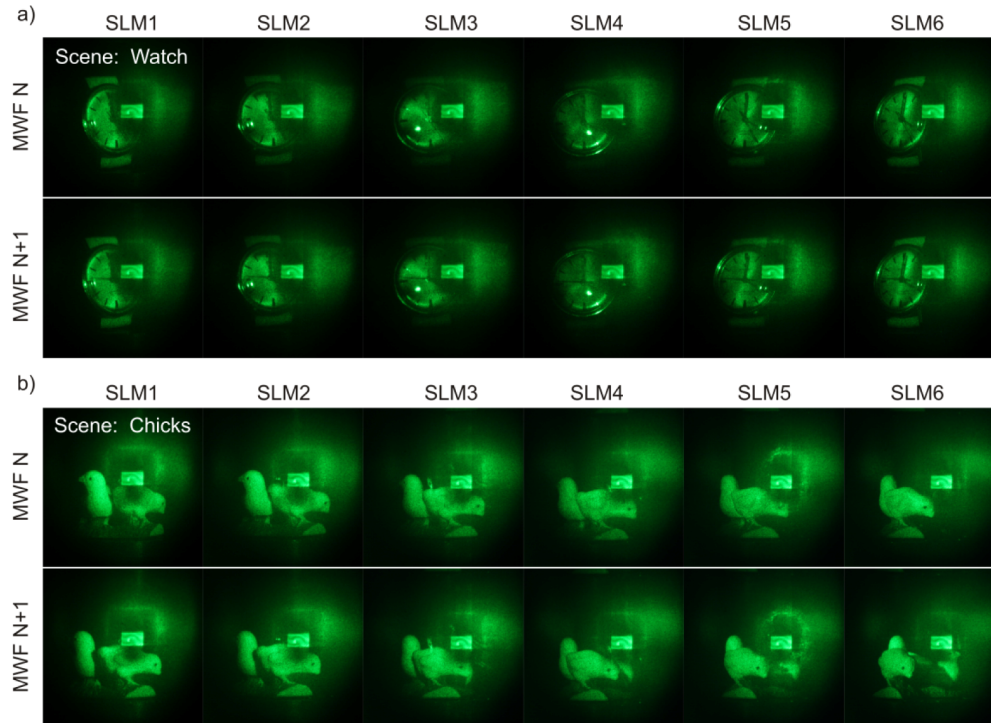


Fig. 9. Images and videos of reconstructions from MWFs by separate SLMs 1-6 for (a) watch ([Media 1](#)) and (b) chicks ([Media 2](#)) objects in the display system acquired during test transfer and the videos of wide viewing angle image of static and running watch combined from all SLMs images ([Media 3](#)).

7. Conclusions

This paper presents for the first time the successful attempt to provide a wide viewing angle holographic television technology path. It gives the full solution of multi wavefront holographic video in which the system is capable of simultaneous capture (Bremen) of six holographic frames of dynamic object and the display system (Warsaw) reconstructing the acquired wavefronts in almost real time. The link between capture and display sites is realized via a transfer - processing platform, which (1) drives capture sensors, (2) compress holograms, (3) sends the data to display side, (4) decompresses holograms, (5) filters holograms, (6) processes them to display geometry and (7) drives display SLMs.

The holographic capture system is built from six DH sensors supplied by reference waves with compact housings aligned on a circle. The solution facilitates a simplified system reconfiguration. The object and reference waves are originating from a single pulse laser with 10 Hz rate, which enables the capture of dynamic scenes, however the limitation of the capture system frame rate should be taken into consideration. The sensors are driven by C++ software which allows for simultaneous capture of all six holograms with pixel numbers matching on the display side. The holograms are coded into a single MWF of pixel dimensions $6 \times 1920 \times 1080$, which is compressed and send via internet. The internet transfer is a frame rate bottle neck and the most optimal of the tested compressions increased frame rate three times (0.38 Hz). Frame compression and decompression is a computationally heavy process and we have found that it limits our system at 1.9 Hz.

The object and reference waves are originating from a single pulse laser with 10 Hz rate, which enables the capture of dynamic scenes, however the capture system limitation of the frame rate should be taken into consideration.

At the capture side the holograms are processed by software running on three GPUs, the data are split and each GPU processes two holograms, the processing includes autofocusing, twin image reduction and tilted plane correction. We have achieved processing frame rate of 2.46Hz, which is mostly determined by the twin image reduction procedure. The procedure is very heavy for in-line holograms. For example using off-axis architecture allowed increasing the processing frame rate to 10.07Hz. The GPU software is responsible for fast and synchronous display of the processed phase distributions.

The holographic display system is built from six SLMs, and its design is driven by the capture configuration, pixel dimensions, wavelengths and orientations of CCDs and SLMs with respect to reference and reconstruction waves. To ensure that the display system reconstructs multiple object wavefronts in mutually correct orientations we have developed a calibration method that finds the relative positions of the CCDs and this data is used for generation of test holograms allowing accurate display calibration before displaying captured holograms.

Finally the experiments had proven the full functionality of the holographic television system. Future work will focus on system configuration and methods that enable a decrease in the gaps between the reconstructed images caused by capturing only a fraction of the object field. We expect that to solve this problem a hybrid opto-numerical solution based on spatio-temporal hologram and object wavefronts multiplexing will be most efficient.

Acknowledgments

The research leading to these results has received funding from the EU 7th Framework Program FP7/2007-2013 under agreement 216105 ('Real 3D' Project) and the statutory funds of Warsaw University of Technology.